Biochemical Pharmacology 78 (2009) 406–413

Contents lists available at ScienceDirect

Biochemical Pharmacology

journal homepage: www.elsevier.com/locate/biochempharm

Evaluation of the binding orientations of testosterone in the active site of homology models for CYP2C11 and CYP2C13

Hongwu Wang, Jemmie D. Cheng, Diana Montgomery, K.-C. Cheng *

Schering-Plough Research Institute, 2015 Galloping Hill Road, Kenilworth, NJ 07033, USA

ARTICLE INFO

Article history:
Received 4 March 2009
Accepted 15 April 2009

Keywords:
CYP2C
Homology modeling
Testosterone metabolism
Substrate docking
CYP binding site

ABSTRACT

Cytochromes P-450 2C11 and 2C13 are the major CYPs in rat liver microsomes. Despite a high degree of sequence identity, these two isozymes display different positional and regio-specific metabolism of steroid hormones, such as testosterone. CYP2C11 converts testosterone to 2α-hydroxyl and 16α-hydroxyl metabolites, while CYP2C13 produces primarily the 6β-hydroxyl metabolite. Using a human CYP2C9 crystal structure as the template, homology models were generated for CYP2C11 and CYP2C13. Despite similar volume of the binding pockets for CYP2C11 and CYP2C13, the models for these two CYPs showed a substantial difference in the shape of the substrate-binding sites. Substrate docking using rigid and induced-fit methods showed that testosterone fits into the substrate-binding sites of both CYP2C11 and CYP2C13 without the need of added constraints. These docking exercises appear to support testosterone binding in both CYP2C11 and CYP2C13. A constrained docking using energy minimization is required to position testosterone for more precise positional and regio-specificity in supporting the observed metabolism. These results demonstrate the complexity of using modeling for understanding the binding of substrate to CYPs, and suggest that, as a complement to the metabolism data, modeling and docking may yield reliable structural information for the molecular interaction between the substrate and the CYPs.

1. Introduction

Liver microsomal cytochromes P-450 (CYP) constitute a large and diverse gene superfamily. These hemoproteins are the enzymes responsible for the metabolism of a large variety of xenobiotics, such as drugs, carcinogens, pesticides, and pollutants [1,2]. They also play an essential role in maintaining the homeostasis of many physiological substrates, such as steroid hormones and bile acids [3]. Among the most common endogenous steroid hormones are androgens, progestins and estrogens. The metabolic pathways responsible for the metabolism of steroid hormones in both animals and humans have been well elucidated. For example, human CYP3A4 converts testosterone primarily to 6β-hydroxyl-testosterone [4]. CYP2C9, on the other hand, showed low catalytic activity in converting testosterone to multiple hydroxylated metabolites and androstenedione [5]. The major isoform in rat liver, CYP2C11, produces 2α-hydroxyl and 16α-hydroxyl-testosterone [6], and CYP2C13, produces 6β-hydroxyl-testosterone. Rabbit CYP2C5 converts progesterone to either 16α or 6β-hydroxyl metabolite [7]. Rats are commonly used in research laboratories as well as in the pharmaceutical industry as the primary rodent species for metabolism and toxicology studies. In rat liver, CYP2C11, similar to CYP3A4 in humans, accounts for about 50% of the total content of rat liver microsomal cytochrome P-450 [8]. The diverse region- and positional specificity of the cytochromes P-450 represents one of the most interesting aspects of the enzymology and structure–function relationship of this group of enzymes. Despite the sequence homology between CYP2C11 and CYP2C13, their region- and positional specificities for testosterone appear to be quiet different.

Recent progress in X-ray crystallography has generated a wealth of information of the 3-dimensional (3-D) structures of mammalian cytochromes P-450 [9–12]. The structures of two members of the CYP2C family, human CYP2C8 and CYP2C9, have been elucidated [13,14]. Since these two enzymes are closely related to the rat CYP2C11 and CYP2C13, they represent suitable templates for homology modeling. These 3-D structures represent snap shots of the conformation of various CYPs. How to relate these snap shots to the complex reaction mechanism of CYPs remains an active and challenging research topic. During the reaction cycle, the substrate binding to the CYP represents the initial step, but not

Abbreviations: CYP, cytochrome P-450; 3-D, 3-dimensional; IFD, induced-fit docking.

* Corresponding author at: Schering-Plough Research Institute, K-15-2-2700, 2015 Galloping Hill Rd, Kenilworth, NJ 07033, USA. Tel.: +1 908 740 4056; fax: +1 908 740 2916.
E-mail address: kuo-chi.cheng@spcorp.com (K.-C. Cheng).

0006-2952/$ – see front matter © 2009 Elsevier Inc. All rights reserved.
doi:10.1016/j.bcp.2009.04.020

necessarily the rate-limiting step for the catalysis [15]. Nevertheless, the binding interaction most likely dictates the location of the oxidation site on the substrate.

Several hypotheses have been proposed with respect to the positional and regio-specificity. For example, multiple binding orientations may provide the opportunity for the production of multiple oxidized metabolites, such as in the case of hydroxylation of progesterone by CYP2C5. This concept only involves a single-step of each binding mode which evokes some induce-fit conformation changes. The other concept involves the multiple-step substrate-binding model, in which the initial substrate binding to the peripheral site followed by subsequent movement toward the active site and interaction with the heme [16]. The central question is whether the X-ray crystal structural information may allow computational examination for the distinct positional and regio-specificity. In this study, we use CYP2C11 and CYP2C13 as models to examine the binding mechanism. The results based on rigid docking, induced-fit docking and energy minimization may shed some light on the positional and regio-specificity of a given substrate.

2. Methods

2.1. Template selection

The amino acid sequences of rat CYP2C11 (UniProt entry P08683) and 2C13 (UniProt entry P20814) were retrieved from the UniProt website [17] and used to search against the PDB database [18] using the Blast method [19]. The pair-wise sequence identities were calculated for 2C11, 2C13, and their homologs. Cyp2C9 was identified as the most homologs to both rat enzymes. Three structures of human CYP2C9 are available from PDB, an apo form (PDB ID: 1og2) and two ligand-bound complexes (PDB ID: 1og5 and 1r9o). The crystal structure with the highest resolution (1r9o) was selected as the template for building the homology model.

2.2. Homology modeling

Homology models of CYP2C11 and CYP2C13 were constructed using the Prime comparative modeling method [20]. The heme and five water molecules were preserved during the model construction. The five water molecules are: 600, 618, 622, 696 and 819 (numbered as in the PDB entry 1r9o) [9]. Based on the 1r9o crystal structure, water 600 forms the sixth coordinate bond with the heme. Waters 618, 622 and 696 form the H-bonding networks around the heme molecule to maintain the structural integrity of the binding pocket. Water 819 forms H-bonds with backbone atoms from residues in the I-helix and induces a kink in the middle of the long helix. This kink is present in all mammalian P450 enzymes [21]. Keeping these water molecules is likely to reduce modeling artifacts introduced in energy minimizations. The Prime loop prediction algorithm was used to generate the conformations in the homology models for the loop regions (aa38–42 and aa214–220) that were absent in the 1r9o structure [22]. Three segments around the missing loops were included for loop prediction: aa36–43 (Loop1), aa69–72 (Loop2) and aa213–221 (Loop3). First, the Serial loop prediction approach with "extend medium" setting was used for the prediction of the conformation of Loop2. Sidechain conformation of amino acid residues within 7.5 Å of the loop was allowed to optimize during the loop prediction. Next, structures of the two missing loops were predicted using the cooperative loop sampling algorithm since their conformations are interdependent. This approach allowed the simultaneous optimization of both loops. Again, sidechain conformation of the residues within 7.5 Å of the two loops was allowed to change. The best loop conformation ranked by Prime energy was retained for further optimization. The model was further refined with sidechain optimization. Finally, Ramachandran plots were generated to verify the quality of the homology model.

The volume of the substrate-binding site was calculated using VOIDOO software [23]. The volume was calculated by rolling a probe with 1.4 Å radius (water) in the active site using the "Probe occupied" option. The heme was treated as part of the protein structure, whereas water molecules were excluded from the calculation.

2.3. Compound preparation

The 3-D structures of testosterone and its metabolites were generated from its two-dimensional structure using the Concord program (Concord software, CA). The structures were then subjected to energy minimization using MacroModel based on Merck Molecular Force Field (MMFFs) and a dielectric constant of 1.0. Energy minimization was terminated with a gradient cut-off of 0.05. The minimized structure was used for the docking exercises.

2.4. Rigid docking

Rigid dockings of testosterone to the CYP2C11 and 2C13 models were carried out using Glide in XP mode [24]. The binding site of each CYP was represented by energy grids using a cubic box centered on the centroid of the cavity. Dimension for the box within which the centroid of a docked pose falls was set to be 12 Å × 12 Å × 12 Å. No geometric or hydrogen-bonding constraint was introduced for substrate docking. A maximum of 10 poses were evaluated for each docking calculation.

2.5. Induced-fit docking (IFD)

The IFD was performed according to the following three consecutive steps [25,26]. First, the ligand was docked into a rigid-receptor model with scaled-down vdW radii (Glide SP mode). A vdW scaling of 0.5 was used for non-polar atoms of both CYP and testosterone. Up to twenty initial ligand poses were retained for subsequent CYP structural refinement. Next, Prime was used to generate the induced-fit protein–substrate complexes. Each of the structures from the previous step was subjected to sidechain and backbone refinement. Any amino acid residue within 5.0 Å of testosterone was included in the refinement. The refined complexes were then ranked by Prime energy. The structures within 30 kcal/mol of the structure with minimal energy were selected for a second round of Glide docking and scoring. Finally, testosterone was re-docked into the refined lower energy CYP structures. An IFD score that accounts for both the protein–substrate interaction energy and the total energy of the system was calculated for ranking the IFD poses. All energy calculations were carried out using the OPLS-2001 force field with implicit solvation model.

2.6. Constrained energy minimization

Testosterone was first manually docked into the binding site of each model. The compound was oriented such that the oxidized hydrogen atom was close to the heme iron while the rest of the entire molecule was fit in the general shape of the active site. A stepwise energy minimization procedure was used to generate the docked structure of each complex. First, a force constant of 100 was applied to constrain the distance between the oxidized hydrogen atom (C2α for CYP2C11 or C6β for CYP2C13) and the ferric atom in the range of 3 ± 1 Å in order to reduce the vdW contacts in the initial manual docking poses. All other non-hydrogen protein atoms were frozen in their initial positions. Minimization was terminated either after 500 steps (PRCG) or when gradient dropped below 0.05. A

second round of energy minimization was carried out under the same conditions as in the first step with the exception that residues located within 5 Å of testosterone were allowed to move freely. The positions of the heme and water molecules within this 5 Å of radius were frozen. Finally, the distance constraint between the hydrogen atom of the oxidized carbon and the ferric atom was removed. The energy minimization was continued until the gradient dropped below 0.05. All energy calculations were carried out with the OPLS-2001 force field.

3. Results

3.1. Testosterone-induced spectral changes of CYP2C11 and CYP2C13

As previously shown (Table 1) [6] testosterone induced two different types of substrate-binding spectra in CYP2C11 and CYP2C13. 2C11 is a high spin cytochrome P-450 in the native oxidized state. Upon binding of testosterone, a high spin to low spin spectral shift was observed previously for CYP2C11 [27]. This conversion may be due to the interaction between either the C3-carbonyl group or the C17-hydroxyl group of testosterone with the ferric atom of the heme. 2C13 is a native low spin form of cytochrome P-450. When CYP2C13 interacts with the testosterone, a low spin to high spin conversion was observed [6]. This change may be due to displacement of a water molecule serving as the distal ligand in the native oxidized ferric form. The substrate-induced spectral changes represent one line of evidence that some direct interaction may happen between the heme and testosterone.

3.2. Testosterone metabolism by CYP2C11 and CYP2C13

As shown previously (Table 2), testosterone is metabolized by purified CYP2C11 to 2α-, and 16α-hydroxyl, and by CYP2C13 to 6β-hydroxyl metabolites [6,28]. The positional and regio-specificity of the metabolism is depicted in Fig. 1. The 3-D structures of the 2α-hydroxyl and 16α-hydroxyl metabolites appear to overlap in a head-to-tail manner when one of the molecules is rotated 180° horizontally (Fig. 1D), suggesting that 2α-hydroxyl and 16α-hydroxyl metabolites could be produced by two super-imposable binding orientations in the substrate-binding site of CYP2C11.

3.3. Homology modeling

Among the CYP enzymes with known crystal structures, the human CYP2C9 is most homologous to rat CYP2C11 and CYP2C13 based on the amino acid sequence. The 2C9 structure (1r9o, with flurbiprofen bound) with the best resolution was selected as the template for the construction of homology models. The sequence identity between CYP2C9 and CYP2C11 or CYP2C13 is 76% or 66%,

Table 1
Spin states of CYP 2C11 and 2C13 and substrate-induced spectral changes by testosterone.

CYP	Spin state	Substrate-induced spectral change	References
2C11	High spin	Reversed type I	[6]
2C13	Low spin	Type I	[6]

Table 2
Hydroxylation of testosterone by CYP 2C11 and 2C13.

CYP	Testosterone	References
2C11	2α, 16α	[6,28]
2C13	6β	[6,28]

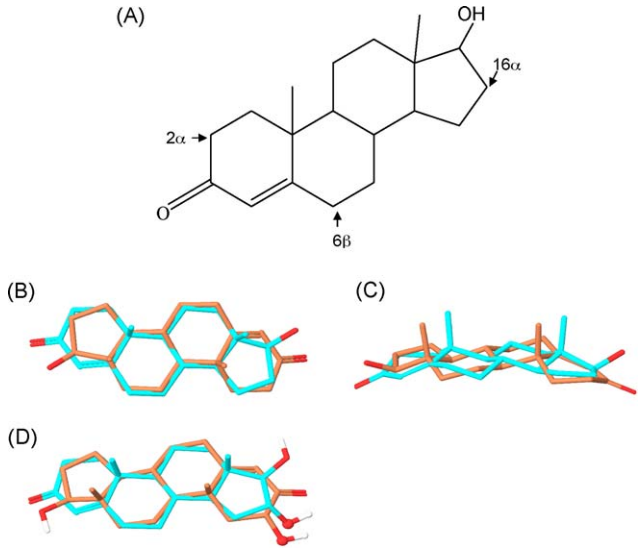

Fig. 1. Structures of testosterone and metabolites: (A) Two-dimensional structure of testosterone with metabolic positions labeled; (B) Top view of overlay of the three-dimensional structure of two testosterone molecules showing the symmetric nature of this compound, blue represents one molecule and orange represents the other molecule; (C) Side view of overlay of the three-dimensional structure of two testosterone molecules (D) Top view of overlay of the 2α-hydroxyl-testosterone and the 16α-hydroxyl-testosterone.

respectively. Fig. 2 shows the sequence alignment of CYP2C11 and CYP2C13 with CYP2C9. The alignment requires neither insertion nor deletion, suggesting a continuation of the structures. The 3-D structure of the homology models for CYP2C11 and CYP2C13 are shown in Fig. 3A. The coordinates of the heme and five water molecules, which were considered to be important for the structural integrity, were copied from the CYP2C9 structure. Fig. 3B and C show the Ramachandran plots for the final CYP2C11 and CYP2C13 models. Only a few residues (<3%), most them glycines, fall into the unfavorable regions on the maps for both models. Since the sequence identities between the 2C9 template and the models of CYP2C11 and CYP2C13 are very high (>60%), the general features of the homology models should be fairly reliable.

3.4. Substrate-binding site

As shown in Fig. 4A, the substrate-binding site of CYP2C11 is characterized by a Phe cluster at the ceiling, similar to that of human CYP3A4. This cluster is composed of six Phe residues: F100, F114, F205, F208, F237 and F476. In contrast, the substrate-binding site of CYP2C13 lacks the Phe residue cluster; four of the six Phe residues were replaced by smaller hydrophobic residues: F100L, F205 V, F208I, and F476L. Two smaller residues in the active site of CYP2C11 are replaced by large amino acids in CYP2C13: V233Y, and G296F; the sidechains of these two residues are located at the top of the cavity, making a larger pocket at the top portion of the binding site for CYP2C11. At the same time, two other residues, located at the bottom of the binding site, in CYP2C11 are replaced by smaller residues in CYP2C13: I113A, and V362G. These residues significantly restricted the shape of the CYP2C11 binding pocket in proximity to the heme compared to that of CYP2C13. The substrate-binding site of CYP2C11 is more hydrophobic than that of the CYP2C13 due to several residue differences: V233Y, F237H, and G447S.

Overall, the binding site of CYP2C11 is slightly larger than that of CYP2C13. When calculated with VIODOO, the volume of the binding cavities of CYP2C11 and CYP2C13 are 556.9 $Å^3$ and 501.5 $Å^3$, respectively. Fig. 4B and C show the surface morphology of the binding sites of CYP2C11 and CYP2C13 models. In the

```
2C9(1r9o) -----------------MAKKTSSGRGKLPPGPTPLPVIGNILQIGIKDI
2C11      MDPVLVLVLTLSSLLLLSLWRQSFGRGKLPPGPTPLPIIGNTLQIYMKDI
2C13      MDPVVVLLLSLFFLLFLSLWRPSSGRGKLPPGPTPLPIIGNFFQVDMKDI

2C9(1r9o) SKSLTNLSKVYGPVFTLYFGLKPIVVLHGYEAVKEALIDLGEEFSGRGIF
2C11      GQSIKKFSKVYGPIFTLYLGMKPFVVLHGYEAVKEALVDLGEEFSGRGSF
2C13      RQSLTNFSKTYGPVYTLYVGSQPTVVLHGYEALKEALVDHGEEFSGRGRL

2C9(1r9o) PLAERANRGFGIVFSNGKKWKEIRRFSLMTLRNFGMGKRSIEDRVQEEAR
2C11      PVSERVNKGLGVIFSNGMQWKEIRRFSIMTLRTFGMGKRTIEDRIQEEAQ
2C13      PICEKVAKGQGIAFSHGNVWKATRHFTVKTLRNLGMGKGTIEDKVQEEAK

2C9(1r9o) CLVEELRKTKASPCDPTFILGCAPCNVICSIIFHKRFDYKDQQFLNLMEK
2C11      CLVEELRKSKGAPFDPTFILGCAPCNVICSIIFQNRFDYKDPTFLNLMHR
2C13      WLVKELKKTNGSPCDPQFIMGCAPGNVICSIILQNRFDYEDKDFLNLIEK

2C9(1r9o) LNENIKILSSPWIQICNNFSPIIDYFPGTHNKLLKNVAFMKSYILEKVKE
2C11      FNENFRLFSSPWLQVCNTFPAIIDYFPGSHNQVLKNFFYIKNYVLEKVKE
2C13      VNEAVKIISSPGIQVFNIFPILLDYCPGNHNIYFKNHTWLKSYLLEKIKE

2C9(1r9o) HQESMDMNNPQDFIDCFLMKMEKEKHNQPSEFTIESLENTAVDLFGAGTE
2C11      HQESLDKDNPRDFIDCFLNKMEQEKHNPQSEFTLESLVATVTDMFGAGTE
2C13      HEESLDVSNPRDFIDYFLIERNQENANQWMNYTLEHLAIMVTDLFFAGIE

2C9(1r9o) TTSTTLRYALLLLLKHPEVTAKVQEEIERVIGRNRSPCMQDRSHMPYTDA
2C11      TTSTTLRYGLLLLLKHVDVTAKVQEEIERVIGRNRSPCMKDRSQMPYTDA
2C13      TVSSTMRFALLLLMKYPHVTAKVQEEIDHVIGRHRSPCMQDRSHMPYTNA

2C9(1r9o) VVHEVQRYIDLLPTSLPHAVTCDIKFRNYLIPKGTTILISLTSVLHDNKE
2C11      VVHEIQRYIDLVPTNLPHLVTRDIKFRNYFIPKGTNVIVSLSSILHDDKE
2C13      MVHEVQRYIDIGPNGLLHEVTCDTKFRNYFIPKGTAVLTSLTSVLHDSKE

2C9(1r9o) FPNPEMFDPHHFLDEGGNFKKSKYFMPFSAGKRICVGEALAGMELFLFLT
2C11      FPNPEKFDPGHFLDERGNFKKSDYFMPFSAGKRICAGEALARTELFLFFT
2C13      FPNPEMFDPGHFLDENGNFKKSDYFIPFSAGKRMCLGESLARMELFLFLT

2C9(1r9o) SILQNFNLKSLVDPKNLDTTPVVNGFASVPPFYQLCFIPIHHHH
2C11      TILQNFNLKSLVDVKDIDTTPAISGFGHLPPFYEACFIPVQRADSLSSHL
2C13      TILQNFKLKSLVDPKDINTTPICSSLSSVPPTFQMRFIPL
```

Fig. 2. Sequence alignment of human CYP2C9, rat 2C11 and 2C13. The amino acid residues which are conserved by all three sequences are represented in shaded pattern.

CYP2C11 model, the upper region of the binding site is wider than the lower region, where the heme is located. On the other hand, the upper region of the binding site of CYP2C13 model is narrower than the lower region.

3.5. Docking of testosterone to CYP2C11

Fig. 5A shows the top ranked rigid docking pose of testosterone to the CYP2C11 model. Testosterone occupies the top 3/4 of the binding cavity, and makes no contact with the heme molecule. In this binding mode, the 3-keto group falls in a pocket close to K108. The distance between the keto O and lysine N atoms is too far for the formation of a direct hydrogen bond, but, favorable electrostatic interaction is clearly possible. The other polar group of testosterone, the 17β-hydroyl group, packs with the sidechains of V362 and F476, and does not make direct polar interaction with CYP2C11. The upper part of the steroid core (where the methyl groups are located) makes beneficial vdW contacts with the Phe cluster at the ceiling of the binding cavity. Two factors most likely dictate the binding orientation of testosterone are the favorable hydrophobic interactions between testosterone and the Phe cluster, and the narrow shape of the binding cavity at the bottom (close to the heme). The closest testosterone hydrogen atom (15α) is 5.4 Å from the heme iron. The 16α-hydrogen is also oriented toward the ferric atom with a distance of 6.2 Å in between. It is possible that by rotating testosterone using the 3-keto as the anchor, the distance between the16α-hydrogen and the iron can be reduced, enabling the oxidation at the 16α position. Most of the IFD models put testosterone at a similar position in the binding cavity as the rigid docking. Furthermore, none of the rigid docking or IFD models put the 2α-hydrogen close to the heme iron. Clearly, for metabolic oxidization to occur at the 2α position, testosterone needs not only move down from the docked position, but also rotate almost 180°.

To get a picture of how the substrate interacts with the enzyme when oxidization occurs at the 2α position, constraint energy minimization was applied to a manually docked model as described in Section 2. During the first two steps of the energy minimization, a distance constraint was applied between the testosterone 2α-hydrogen and the ferric atom. This constraint was removed at the final step of the energy minimization. The minimized model provides a snapshot of the binding orientation and interactions between testosterone and CYP2C11. In this model (Fig. 5B), the 3-keto group dips into the bottom of the binding cavity; the 17β-hydroxyl group makes hydrogen bond with the K108 sidechain and the backbone carbonyl of G296. The 2α-hydrogen is the closest atom from testosterone to the heme iron with a distance of 4.1 Å. Compared to the original CYP2C11 structure, the G296 backbone rotated about 120° and its carbonyl formed a hydrogen bond with the 17β-hydroxyl group. V362 rotated to create slightly larger space and enabled the 3-keto to access the bottom of the cavity. Large changes were not observed

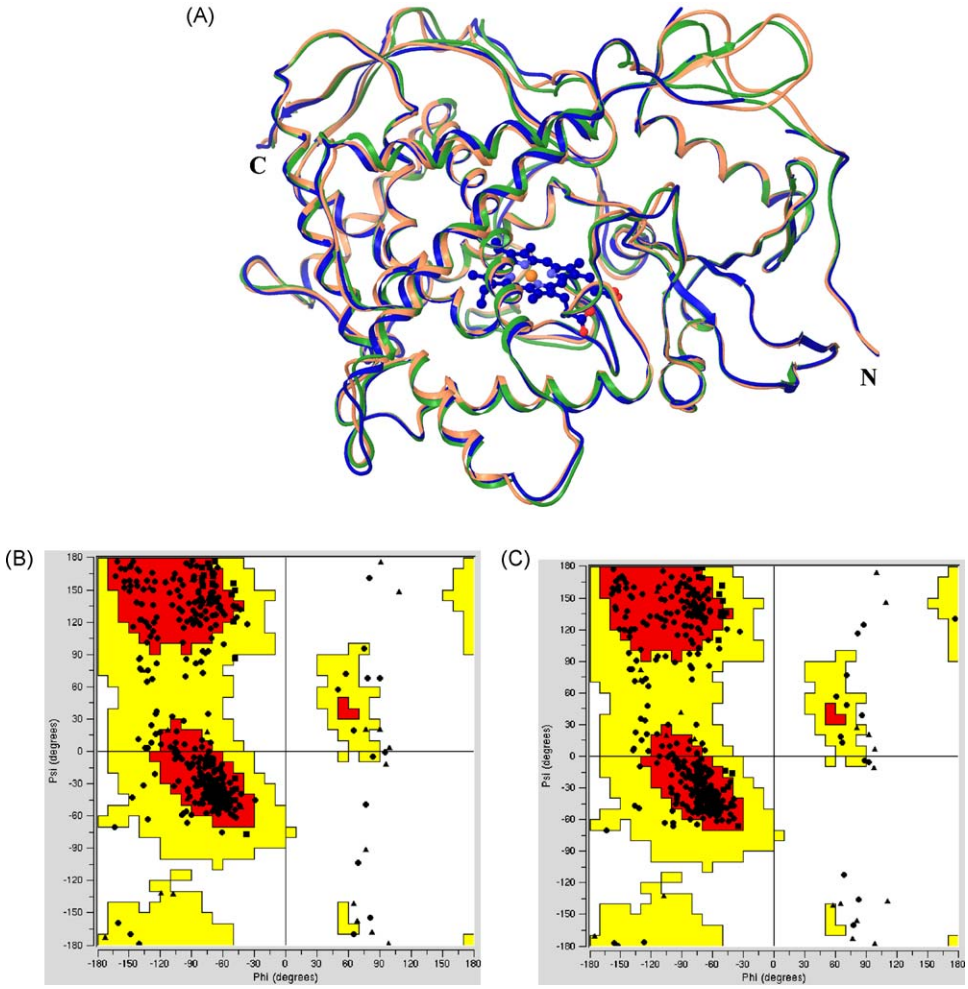

Fig. 3. Homology models for 2C11 and 2C13. (A) Overlay of the homology models and the template (PDB ID: 1r9o) structure. Blue color ribbon represents the 2C9 crystal structure. Brown ribbon represents the 2C11 model, while green ribbon represents the 2C13 model. (B) and (C) Ramachandran plots of the homology models. Triangles on the plots represent Gly residues.

for other residues in the protein active site. The steroid core still maintained favorable hydrophobic interactions with the binding cavity.

3.6. Docking of testosterone to CYP2C13

Fig. 6A shows the rigid docking pose of testosterone to the CYP2C13 model. In this docking pose, the testosterone molecule occupies the lower portion of the binding site, the steroid core makes favorable hydrophobic interactions with some hydrophobic sidechains lining the binding cavity. The 3-keto group forms a hydrogen bond with the sidechain of K108. No hydrogen bond was formed between the 17β-OH and the enzyme. The 11α and 12β H atoms are closest to the ferric atom, with a distance of 3.7 Å and 3.8 Å, respectively. The 6β position is oriented toward the ceiling of the binding site, pointing away from the iron. Most of the IFD models put testosterone at a similar position in the binding cavity as the rigid docking. None of the rigid docking or IFD models put the 6β-hydrogen close to the heme iron. The strong hydrogen bonding interaction between the 3-keto group and K108 anchors the molecule and constrains its movement.

Similar to the situation with CYP2C11, in order to orient the 6β position closer to the reactive center, the molecule needs to rotate ~180° from the rigid docking position. To examine the substrate–protein interactions in the productive mode, a constrained energy minimization was carried out for this system as well. Fig. 6B shows the energy minimized model. In this model, no hydrogen bond was formed between testosterone and CYP2C13. Instead, the 3-keto group makes favorable electrostatic interactions with a polar patch on the binding pocket formed by the backbone of L361 and G362, while the 17β-OH makes favorable electrostatic interactions with the sidechain of R97. The protein conformation did not change much, only minor sidechain movements of K108, F114, F296 and L366 were observed. These sidechain movements fine-tune the shape of the binding site and make it able to better accommodate the new orientation. The 6β-hydrogen now is the closest atom to the heme iron, only 3.3 Å away. The larger volume at the bottom of the binding pocket in CYP2C13 makes its heme iron more accessible to the substrate.

4. Discussion

Previous studies on the kinetics and thermodynamics of substrate binding to cytochromes P-450 suggested that the initial binding of the substrate appears to be located at a peripheral site that may not perturb of the heme spectrum [16]. Subsequent substrate movement toward the heme and in conjunction with the conformation change occurring at the substrate-binding site may contribute to the spectral change of the heme (high spin to low spin or low spin to high spin change). Although the peripheral binding site could be further away from the heme, it is also conceivable that this initial site could be located within or with close proximity to

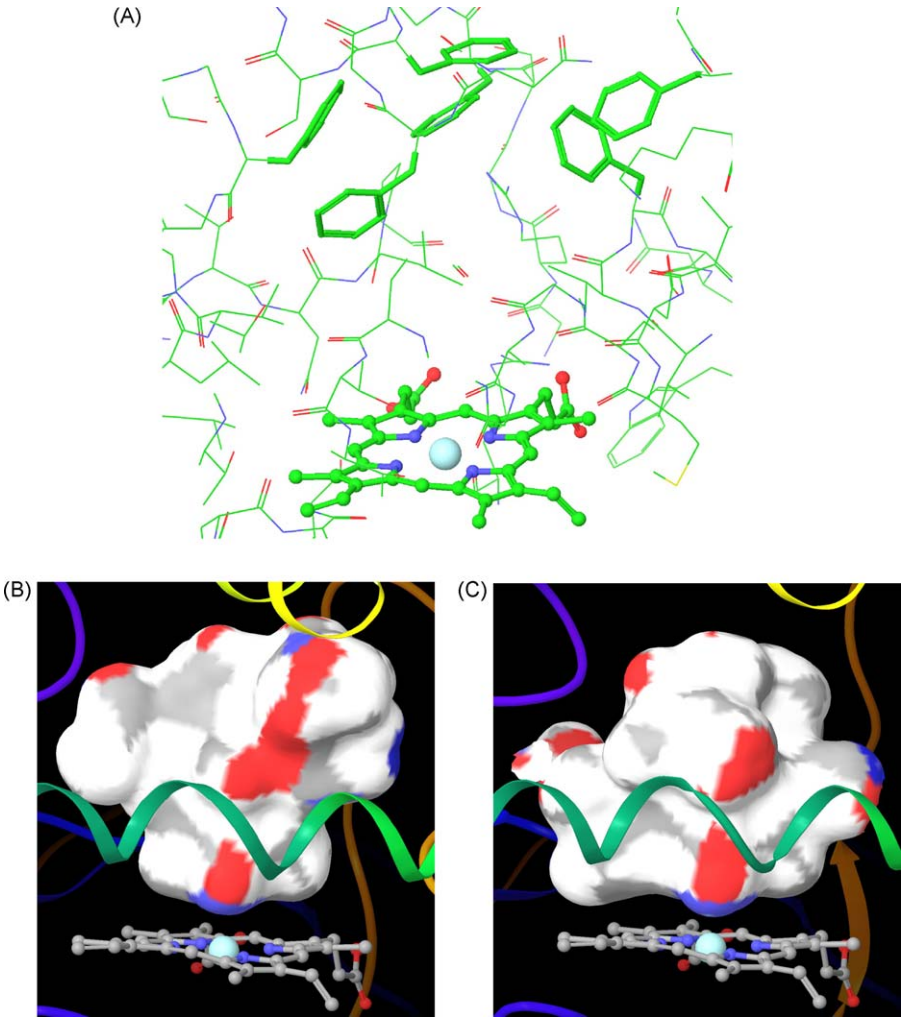

Fig. 4. The Phe cluster in the CYP 2C11 active site (A) and the shapes of 2C11 (B) and 2C13 (C) binding pockets. The helix shown in front is Helix I. The surfaces are colored by the atom types (H: white; C: gray, O: red and N: blue) of the contacting protein atoms.

the substrate-binding site. Under this scenario, the mechanism that enables the substrate to move from the initial binding to productive mode may involve some kind of conformational changes in the substrate-binding site. This transition model concept is supported by the CYP2C5 crystal structure [29]. The substrate–CYP2C5 complex suggested that the flexible regions of the protein are adaptive for substrate binding with conformational changes contributing to more favorable binding interaction. In addition, the substrate used in that study appears to bind in two distinct, overlapping locations of which only one leads to extensive oxidation. Alternatively, the one step induced-fit model as implied by most modeling studies appears to position the substrate directly at the proximity of the heme for the formation of productive substrate–CYP complex. According to this hypothesis, the initial binding, the conformation change due to induce-fit, and the heme spectral change may happen simultaneously.

The chemistry of catalysis of cytochrome P-450 monoxygenase is a complex and multi-step phenomenon [1]. The catalytic cycle consists of steps related to binding of the substrate, the activation of oxygen, followed by substrate oxidation and product release. Which of these steps is rate-limiting depends upon the enzyme, the substrate, and the specific reaction. Although considerable research has focused on the mechanism of CYP reactions, significant interests remain in the substrate-binding site and the binding orientation of the substrate since this step may dictate the positional and regio-specificity of the substrate metabolism.

In this study, we used a human CYP2C9 crystal structure as the template for building the homology models of two major rat CYPs, CYP2C11 and CYP2C13. Docking experiments using rigid and induce-fit conformations showed the binding of testosterone to CYP2C11 with the oxidation site at relatively remote distance of 6–7 Å from the center ferric atom of the heme. This distance may be too far to allow the catalysis to occur as proposed by several studies [30]. It is possible that the crystal structure is more restricted than the aqueous structure during the actual catalysis. Hence, with a more open and flexible aqueous structure it would allow the steroid substrate to better orient in the substrate-binding cavity. In additional docking experiments using the energy minimization method, testosterone is locked into a distance constraint between the oxidized carbon and the ferric atom of the heme. This exercise becomes feasible with the information regarding the positional and regio-specific metabolism of testosterone. A comparison between the testosterone binding conformations derived from rigid/induce-fit and the energy minimization provides a glimpse with respect to the orientation of testosterone in the substrate-binding site. Only a minor conformational change in the CYP2C11 binding site and a rotation of testosterone would be needed for these two conformers. Similarly, for CYP2C13 both induced-fit and energy minimization docking exclude the potential formation of either 2α- or 16α-hydroxyl metabolite. However, the binding conformation predicted by the induced-fit docking will require a significant rotation of the molecule in order to orient the 6β-

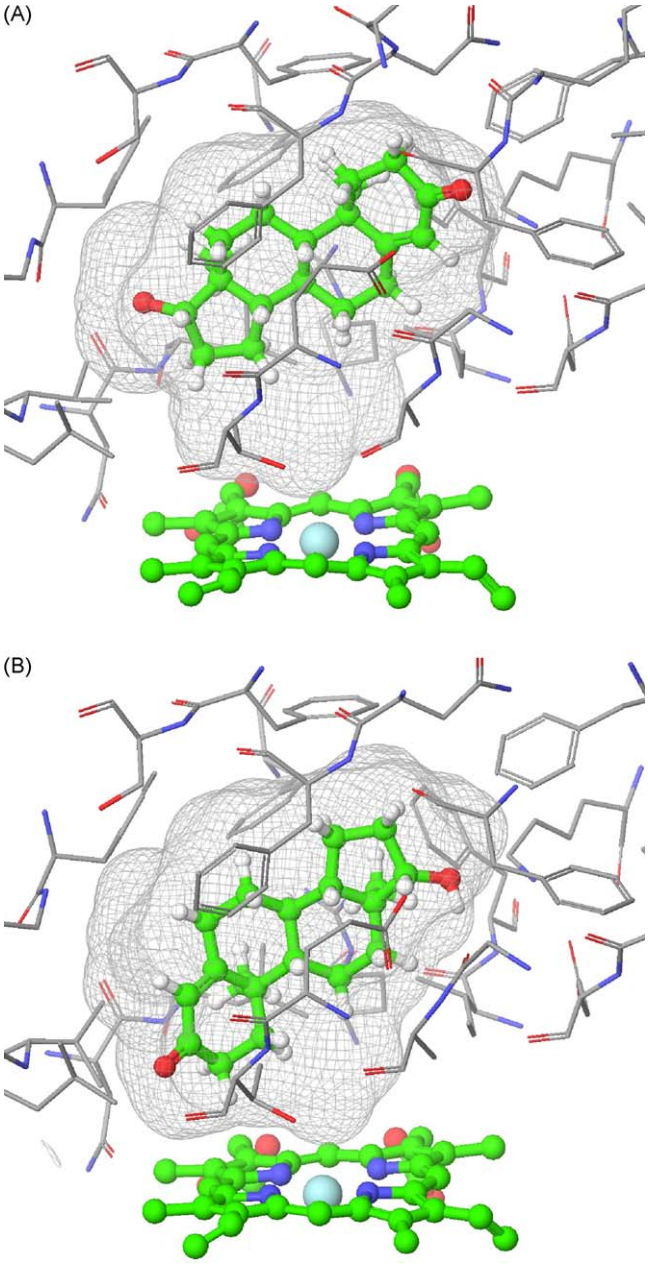

Fig. 5. Docking of testosterone to CYP2C11. (A) Rigid docking showing the location of the initial binding site of testosterone in 2C11. The top ranking binding mode in rigid docking showing 16α position is the closest to heme iron, but not close enough for oxidative interactions. (B) Constraint energy minimization structure.

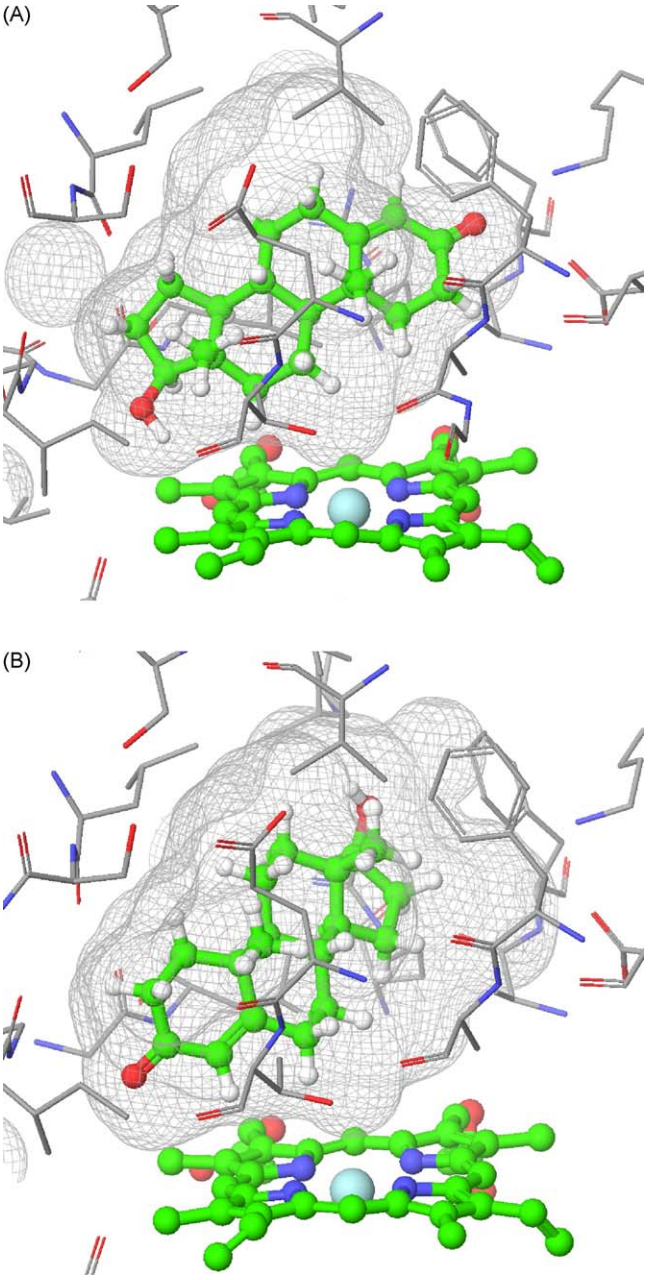

Fig. 6. Docking of testosterone to CYP2C13. (A) Rigid docking showing the location of the initial binding site of testosterone in 2C13. The top ranking binding mode in rigid docking showing 6β position is far away form heme iron. (B) Constraint energy minimization structure.

position toward the heme. Our results appear to support the transition model, in such that the rigid/induce-fit conformation represents the initial binding of the substrate, whereas the energy minimization conformation represents the productive binding mode of the substrate–CYP complex.

Recent advances in the structural elucidation of the hepatic microsomal CYPs have generated a wealth of information on the three-dimensional structures of various isoforms. Incorporation of such information into the kinetics of substrate binding appears to be useful, yet the utility is not totally clear with respect to the prediction of catalytic rate and the positional and regio-specificity of the oxidative reaction [31]. Due to the large number of substrates available, examination of the substrate binding, the interaction between the enzyme and the substrate, and the orientation of the substrate by using structural modeling tools has become a necessity. While the need for using the structural modeling information, especially, in lead optimization in the drug discovery process becomes essential, various challenges underscore the feasibility primarily due to the flexible and large binding cavity of various CYPs. As presented in this study, it demonstrates the complexity of using modeling for understanding the binding of substrate to CYPs, and suggests that, as a complement to the metabolism data, modeling and docking may yield reliable structural information for the molecular interaction between the substrate and the CYPs.

References

[1] Guengerich FP. Uncommon P450-catalyzed reactions. Curr Drug Metab 2001;2:93–115.

[2] Rendic S. Summary of information on human CYP enzymes: human P450 metabolism data. Drug Metab Rev 2002;34:83–448.
[3] Leblanc GA, Waxman DJ. Feminization of rat hepatic P-450 expression by cisplatin-Evidence for pertubations in the hormonal regulation of steroid-metabolizing enzymes. J Biol Chem 1988;263:15732–9.
[4] Kawano S, Karnataki T, Yasumori T, Yamazoe Y, Keto R. Purification of human liver cytochrome P-450 catalyzing testosterone 6β-hydroxylation. J Biochem 1987;102:493–501.
[5] Yamazaki H, Shimada T. Progesterone and testosterone metabolism by cytochromes 2C19, 2C9 and 3A4 in human liver microsomes. Arch Biochem Biophys 1997;346:161–9.
[6] Cheng KC, Schenkman JB. Testosterone metabolism by cytochrome P-450 isozymes RLM3 and RLM5 and by microsomes. Metabolite identification. J Biol Chem 1983;258:11738–44.
[7] Williams PA, Cosme J, Sridhar V, Johnson EF, McRee DE. Mammalian microsomal cytochrome p450 monooxygenase: structural adaptations for membrane binding and functional diversity. Mol Cell 2000;5:121–31.
[8] Evans WE, Relling MV. Pharmacogenomics: translating functional genomics to rational therapeutics. Science 1999;286:487–91.
[9] Wester MR, Yano JK, Schoch GA, Yang C, Griffin KJ, Stout CD, et al. The structure of human cytochrome p450 2c9 complexed with flurbiprofen at 2.0-a resolution. J Biol Chem 2004;279:35630–7.
[10] Williams PA, Cosme J, Vinkovic DM, Ward A, Angove HC, Day PJ, et al. Crystal structures of human cytochrome P450 3A4 bound to metyrapone and progesterone. Science 2004;305:683–6.
[11] Ekroos M, Sjogren T. From the cover: structural basis for ligand promiscuity in cytochrome P450 3A4. Proc Natl Acad Sci USA 2006;103:13682–7.
[12] Schoch GA, Yano JK, Sansen S, Dansette PM, Stout CD, Johnson EF. Determinants of cytochrome P450 2C8 substrate binding: structures of complexes with montelukast, troglitazone, felodipine, and 9-cis-retinoic acid. J Biol Chem 2008;283:17227–3.
[13] Williams PA, Cosme J, Ward A, Angove HC, Vinkovic DM, Jhoti H. Crystal structure of human cytochrome P450 2C9 with bound warfarin. Nature 2003;424:464–8.
[14] Schoch GA, Yano JK, Wester MR, Griffin KJ, Stout CD, Johnson EF. Structure of human microsomal cytochrome P450 2C8: evidence for a peripheral fatty acid binding site. J Biol Chem 2004;279:9497–503.
[15] Guengerich FP. Cytochrome P450: what have we learned and what are the future issues? Drug Metab Rev 2004;36:159–97.
[16] Isin EM, Guengerich FP. Multiple sequential steps involved in the binding of inhibitors to cytochrome P-450 3A4. J Biol Chem 2007;282:6863–74.
[17] The UniProt Consortium. The universal protein resource (UniProt). Nucl Acids Res 2008;36:D190–5.
[18] Berman HM, Westbrook J, Feng Z, Gilliland G, Bhat TN, Weissig H, et al. The protein data bank. Nucl Acids Res 2000;28:235–42.
[19] Altschul SF, Gish W, Miller W, Myers EW, Lipman DJ. Basic local alignment search tool. J Mol Biol 1990;215:403–10.
[20] Andrec M, Harano Y, Jacobson MP, Friesner RA, Levy RM. Complete protein structure determination using backbone residual dipolar couplings and side-chain rotamer predication. J Struct Funct Genom 2002;2:103–11.
[21] Locuson CW, Tracy TS. Identification of binding sites of non-i-helix water molecules in mammalian cytochromes P450. Drug Metab Dispos 2006;34:1954–7.
[22] Zhu K, Shirts MA, Friesner RA. Improved methods for side chain and loop predictions via the protein local optimization program: variable dielectric model for implicitly improving the treatment of polarization effects. J Chem Theory Comput 2007;3:2108–19.
[23] Kleywegt GJ, Jones TA. Detection, delineation, measurement and display of cavities in macromolecular structures. Acta Cryst Sec D 1994;50:178–85.
[24] Friesner RA, Banks JL, Murphy RB, Halgren TA, Klicic JJ, Mainz DT, et al. Glide: a new approach for rapid, accurate docking and scoring. 1. Method and assessment of docking accuracy. J Med Chem 2004;47:1739–49.
[25] Sherman W, Day T, Jacobson MP, Friesner RA, Farid R. Novel procedure for modeling ligand/receptor induced fit effects. J Med Chem 2006;49:534–53.
[26] Nabuurs SB, Wagener M, de Vlieg J. A flexible approach to induced fit docking. J Med Chem 2007;50:6507–18.
[27] Licas-Coles E, He K, Yin H, Correia MA. Cytochrome P450 2C11: *E. coli* expression, purification, functional characterization, and mechanism-based inactivation of the enzyme. Arch Biochem Biophys 1997;338:35–42.
[28] Cheng KC, Schenkman JB. Metabolism of progesterone and estradiol by microsomes and purified cytochrome P-450 RLM3 and RLM5. Drug Metab Dispos 1984;12:222–34.
[29] Cosme J, John EF. Engineering microsomal cytochrome P-450 2C5 to be a soluble, monomeric enzyme mutations that alter aggregation, phospholipids dependence of membrane binding and catalysis. J Biol Chem 2000;275:2549–53.
[30] Jovanovic T, Farid R, Friesner RA, McDermott AE. Thermal equilibrium of high- and low-spin forms of cytochrome P450 BM-s: repositioning of the substrate. J Am Chem Soc 2005;127:13548–52.
[31] Ekins S, de Groot MJ, Jones JP. Pharmacophore and three-dimensional quantitative structure activity relationship methods for modeling cytochrome P450 active sites. Drug Metab Dispos 2001;29:936–41.